



Runoff assessment in the Padma River Basin, Bangladesh: a GIS and RS platform in the SCS-CN approach

Md. Tareq Aziz¹ · Md. Rabiul Islam¹ · Zarjes Kader¹ · H. M. Imran¹ · Manik Miah¹ · Md. Rakibul Islam¹ · Majmumas Salehin¹

Received: 14 December 2022 / Revised: 31 March 2023 / Accepted: 1 April 2023 / Published online: 11 April 2023
© The Author(s), under exclusive licence to Springer Nature Switzerland AG 2023

Abstract

Rainfall and runoff are the essential hydrologic parameters when estimating water resources. This study aims at estimating surface runoff on the Padma river basin based on the SCS-CN method in a geographic information system (GIS) and remote sensing (RS) environment. The SCS-CN is, however, one of the most widely used runoff estimation method, and its critical features i.e., the runoff curve number (CN) depends greatly on land use and land cover (LULC), soil type, and antecedent soil moisture (AMC). In addition, to make it viable in runoff estimation, it requires some other crucial parameters, e.g., hydrological soil characteristics (HSG), precipitation (P), potential maximum retention, antecedent moisture condition (AMC), and weighted curve number (WCN). The daily runoff of the Padma river basin has, therefore, been estimated for the period 2010–2020, and an average annual surface runoff of 409.67 mm was found in this study, i.e., equivalent to 12.6×10^3 m³ in volume and representing about 22.25% of the total average annual rainfall. Here, some non-parametric statistical tools, for example, statistical autocorrelation, Mann–Kendall, and Sen slope, were used to investigate the monthly surface runoff trends. According to the Mann–Kendall method, statistically significant monotonic trends were found. Smoothing curve analysis reveals that the monthly mean runoff is 34 mm. The degree of effect of several land use patterns with corresponding soil types was analyzed to assess the total runoff volume contributing to the surface water resources.

Keywords Rainfall · Overland flow · GIS · Remote sensing · Man–Kendell · Sen slope

1 Introduction

Water is used in many ways in our environment that benefit us directly or indirectly. Humans' most important water uses are industry, drinking, agriculture, energy production, and transportation. Every piece of land on the planet's surface is part of a watershed or river basin formed by water flowing over and through it (Bhat et al., 2019). Every river basin is a hydrological unit selected by natural ridges that allow drainage in a well-defined drainage pattern of streams running within the limits of the watershed's runoff from rainfall (Bhat et al., 2019). Water is the most important resource on the planet and has long been regarded as a rare natural

resource and a valuable component in global socioeconomic development (Bal et al., 2021). The freshwater supply could significantly decline in the coming decades due to accelerating population growth, surface water pollution, and climate change. Assessing and conserving surface water supplies is vital to assure subsistence in light of the aforementioned issues (Bal et al., 2021; Soulis, 2021). Around the world, there are more and more severe water shortages. Most of the world is divided into arid and semi-arid regions. Due to a scarcity of water resources, these places commonly endure interrupted draughts and water crisis issues (Zehtabiyane-Rezaie et al., 2019). Additionally, irregular and insufficient precipitation, floods, soil erosion brought on by heavy rainfall, and a high rate of surface drainage are frequent occurrences (Piacentini et al., 2018). To meet many requirements, including those for agriculture, hydropower, industries, the climate, and environmental systems, rainfall is the main source of runoff (Ogden et al., 2017; Rizeei et al., 2018). Water resources are necessary for recharging groundwater in the watershed through rainfall and runoff (Satheeshkumar

Communicated by M. V. Alves Martins

✉ Md. Rabiul Islam
mriceduet@gmail.com

¹ Institute of Water and Environment, Dhaka University of Engineering and Technology, Gazipur 1707, Bangladesh

et al., 2017a). The management of water resources requires a systemic approach that considers all hydrological elements as well as the connections, ties, interactions, effects, and consequences that these elements have (Al-Ghobari & Dewidar, 2021). Runoff is a crucial hydrologic element in assessing water resources (Ibrahim et al., 2021). Runoff is the flow of precipitated water down a basin stream after the surface and subsurface losses have been met. River basin characteristics like length, width, area, form, drainage design, soil type, plant cover, land use, and hydrological conditions significantly impact the rainfall-runoff process (Caletka et al., 2020). Runoff is the term used to describe the excess water, sediment, and rocks that flow over the stream channel's surface after evaporation. Rainfall characteristics, including intensity, duration, and dispersion, are important factors influencing the occurrence and measurement of runoff. The link between precipitation amount and considerable runoff is typically determined by soil infiltration. The rainfall-runoff connection is quite complicated, and it is impacted by a variety of storms and channel properties (Lian et al., 2020; Verma et al. 2020). Runoff is produced by rainfalls and it directly impacted by the amount, timing, and distribution of the rainfall event. In addition to these qualities of rainfall, a number of catchment-specific factors influence the runoff frequency and amount. (Jahan et al., 2021). A vital component in the creation of hydraulic structures and erosion control systems would be discharge which generated by rainfall in a watershed or river basin (Deshmukh et al., 2013).

However, the logical approach, the Green Ampt method, and the Soil Conservation Service-Curve Number (SCS-CN) method are only a few available methods for determining runoff (Jaafar et al., 2019). The SCS-CN approach was created in 1969 by the National Resources Conservation Service (NRSC), a division of the United States Department of Agriculture (USDA). This method calls for using a straightforward empirical formula and widely accessible tables and curves. A high density of curves in metropolitan settings suggests heavy runoff and minimal infiltration, whereas a low density indicates light runoff and substantial infiltration in dry soil (Shadeed & Almasri, 2010). Based on storm rainfall depth, it is a straightforward, reliable, and stable conceptual method for measuring direct runoff depth. This method relies on numerical catchment features to calculate runoff. Land use, hydrologic condition, agricultural management, soil moisture, and distribution of soil types are the main factors in rainfall-runoff analyses. Four Hydrologic Soil Groups (HSG) are created by classifying Group A, B, C, and D soil types. The "Category A" hydrologic soil group's soil types have a high infiltration rate. On the other hand, soil with a poor infiltration rate is included in hydrologic soil the "Group D". The planning, development, and management of water and natural resources may all be aided

using geographic information system (GIS) and remote sensing (RS) techniques. The synoptic perspective and thorough coverage offered by remote sensing satellite photography might benefit every river basin. The GIS environment enables decision making through geographic analysis and the fusion of many thematic data sets into a single platform. Due to their synergy, RS and GIS are essential in hydrological applications; a hydrologist may create a cohesive use case (Balkhair & Ur Rahman, 2021; Karimi & Zeinivand, 2021; Rana & Suryanarayana, 2020). The GIS framework enables rapid acquisition, evaluation, and interpretation of multidisciplinary data on a large scale using remote sensing, which is extremely useful for watershed planning. Using traditional methods for estimating runoff capacity in unmeasured watersheds involves extensive effort and time. Most traditional methods of runoff calculation are complicated and expensive for small watersheds in difficult terrain (Farooq et al., 2021; Pandey et al., 2013). A runoff data analysis is essential for preserving and expanding natural assets. As a result of the availability of geographic datasets, hydrological applications are using them more frequently. A geospatial system has evolved into an essential hydrologic modeling tool because it is highly efficient in producing geographically dispersed model parameters (Bera & Singh, 2021; Farooq et al., 2021). This case study used the SCS-CN model, Mann-Kendall (modified for Indian conditions), a conventional database, and GIS techniques to predict surface runoff in the Padma River basin. The Mann-Kendall and Sen slopes were used to evaluate this runoff and find trends in the watershed runoff data set. The Mann-Kendall method is the most popular non-parametric technique for identifying monotonic trends in hydrological parameter data (Bhat et al., 2019; Kendall, 1975; Mann, 1945; Pastor et al., 2013; Rashid et al., 2013; Renard et al., 1994).

Estimates of surface runoff are important in the Padma River basin. In the study region, agriculture predominates over all other land use and land-cover classifications, with several others present (Arefin et al., 2021; Islam et al., 2021). The fallow and open shrub land use types are the most significant for surface runoff. For calculating runoff potential, the hydrologic soil group—which represents the soil type, category, and infiltration capability—is very helpful (Kumar et al., 2021). Managing and evaluating water resources depend on accurate information on runoff volumes. Numerous factors, such as precipitation type, duration, volume, and intensity, impact runoff amounts. The basin type also affects the amount of runoff (Sorucu et al., 2015). Land development typically results in impermeable zones that enhance storm runoff. Usually, evolution must eliminate native vegetation and level the terrain to increase the amount of rain that falls (Shao et al., 2019). The leaves of natural vegetation collect precipitation, which is then absorbed by the plants' roots. Uneven surfaces increase surface friction,

which prolongs the time that raindrops remain on the surface until they drain (Fausey, 2004). Usually, evolution must eliminate native vegetation and level the terrain to increase the amount of rain that falls. The leaves of natural vegetation collect precipitation, which is then absorbed by the plants' roots. Uneven surfaces increase surface friction, which prolongs the time that raindrops remain on the surface until they drain (Al-Ani et al., 1971). As a result, surface infiltration decreases, and impermeable surfaces increase as development progresses (Lobo et al., 2004). In the analysis of river basins, impermeable surfaces result in an increase in runoff and a decrease in groundwater recharge, leading to an increase in river overflow and the potential of flooding during storms.

The Padma is one of the three major rivers in Bangladesh, so estimating the surface runoff in the river's basin is crucial. Recently, the basin has suffered from a deficiency of rainfall, resulting in a drought-like condition and abnormally excessive runoff at different times of the year. In this basin, cropland and managed vegetation are found as the predominate land use classes, although fallow land and open shrub land are the land use types that positively contribute to the runoff volume. In addition, the hydrologic soil group representing the soil character, category, and capability of infiltration plays a key role in runoff phenomena in the runoff estimation process. However, to ensure the best management and evaluation practice of water resources, quantifying the potential runoff volumes is crucial, taking into account the characteristics of the rainfalls such as type, duration, volume, and intensity. The author was inspired to estimate the potential runoff of the Padma river basin because no prior study had been conducted here. Thereby, this study aims at predicting the potential runoff using the widely used SCS-CN method in a robust geospatial technique like a GIS platform and exploring the statistical characteristics of the runoff patterns.

2 Materials and methods

2.1 Study area

The basin of the Padma River is located in the middle part of Bangladesh, and the geographical location of this study area is between 89°36'0" and 89°45'0" E longitudes and 23°48'0" to 24°4'0" N latitude, with a total area of 178.871 km² (Fig. 1). The study area is situated on the north, east, and west sides of the districts of Rajbari, Pabna, and Manikgonj, respectively. Where many highland streams feed it. The Padma River's flow pattern has been significantly altered due to the construction of buildings, increased urbanization and industrialization, and expansions in agriculture within the basin (Raihan et al., 2021). As a result, the discharge rate has dropped, particularly during the dry season. The

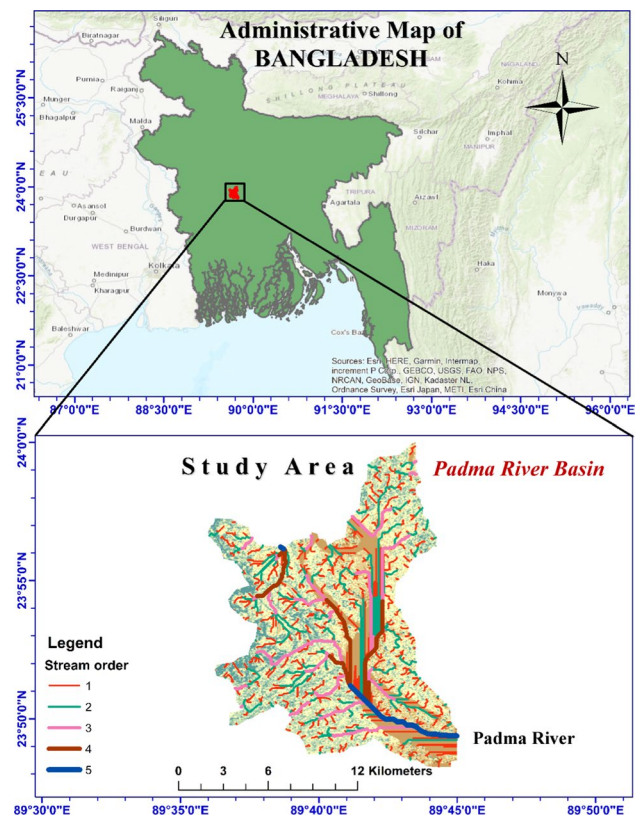


Fig. 1 Location map of the study area

monthly temperature cycle in the basin is governed by the monsoon, with December and January typically being the coldest months at approximately 16–20 °C and May–August typically being the warmest at around 38–40 °C. The annual average rainfall is around 1840 mm, most of it falling during the summer monsoon (June–September) (Raihan et al., 2020). During the monsoon season, the river is prone to flash floods due to excessive rainfall.

2.2 Data used

In this study, the daily precipitation data from 2010 to 2020 were downloaded from the Data Access Viewer, NASA POEWER. The Hydrologic Soil Group (HSG) was obtained from the ORNL DAAC. The SRTM-Digital Elevation Mode (DEM) was downloaded from USGS Earth Explorer to prepare various thematic maps of the study area. However, a detailed list of the data used in the current study is presented in Table 1.

Table 1 Sources of the data sets

SN	parameters	Scale/spatial resolution	Temporal scale	Data format	Sources
1	Precipitation	–	2010–2020	CSV	Data Access Viewer (DAV)- NASA POWER https://power.larc.nasa.gov/data-access-viewer/
2	Land use and land class (LULC)	10 m × 10 m	2020	Geotiff	Esri 10-Meter Land Cover https://www.arcgis.com/apps/mapviewer/index.html?layers=d6642f8a4f6d4685a24ae2dc0c73d4ac
3	Hydrologic Soil Group (HSG)	250 m × 250 m	2020	Geotiff	ORNL DAAC https://daac.ornl.gov/cgi-bin/dsvviewer.pl?ds_id=1566
4	SRTM-Digital Elevation Mode (DEM)	30 m × 30 m	2020	Geotiff	USGS Earth Explorer https://earthexplorer.usgs.gov/

2.3 Methodology

2.3.1 SCS-CN model

The amount of direct runoff that may occur in a river basin due to rainfall may be calculated using various hydrologic models (Walega et al., 2020). With various input data types and circumstances, these models range from complex to basic. Basin characteristics and intricate physical patterns are coupled with straightforward empirical formulas to estimate runoff in the basin (Verma et al., 2021). Numerous users, such as irrigation engineers, environmentalists, and hydrologists, use the SCS-CN to model and compute surface runoff from precipitation (Kumar & Jhariya, 2017; Shi & Wang, 2020; Verma et al., 2020a). For evaluating direct runoff, the SCS model is frequently employed. The much more crucial phase of runoff measurement is the identification and calculation of the stream/drainage area of the river basin (Silva & Oliveira, 1999). The SCS-CN technique is the most commonly used experimental method for assessing direct runoff from a watershed (United States Department of Agriculture) (USDA 1999). The SCS-CN method is usually used to calculate the relationship between runoff volume and rainfall volume. The SCS-CN approach can elucidate the water balance equation, as shown below.

$$Q = \frac{(P - I_a)^2}{(P - I_a + S)} \quad (1)$$

Q , P , I_a , and S stand for runoff depth, rainfall depth, initial abstraction, and basin storage, respectively. All units of depth are in mm. where; A variety of hydrologic models can be used to calculate the amount of direct runoff that may occur in a river basin due to rainfall. These

models range from basic to complex in terms of input data types and circumstances. Basin characteristics and intricate physical patterns are coupled with straightforward empirical formulas to estimate runoff in the basin (Verma, Singh, et al., 2020b). Numerous users, including irrigation engineers, environmentalists, and hydrologists, use the SCS-CN model to calculate surface runoff from precipitation (Kumar & Jhariya, 2017). The SCS model is frequently used to evaluate direct run off. Identifying and calculating the drainage area is a much more important phase of runoff measurement.

The amount of precipitation that falls onto the ground surface before the commencement of runoff is known as “initial abstraction” and is often estimated to be 0.2 S (Ling et al., 2020):

$$Q = \frac{(P - 0.2S)^2}{(P + 0.8S)} \quad (2)$$

Here, S is the function of CN .

$$S = \frac{(25400 - 254)}{CN} \quad (3)$$

The hydrologic soil group (HSG) is divided into four groups (A, B, C, and D) based on the soil infiltration rate in the basin area (Rahman et al., 2018). Based on the limitations for precipitation throughout the dormant and growing seasons, the antecedent moisture condition (AMC) is categorized into three types (AMC I, AMC II, and AMC III). In this case, the CN value was derived from the technical release. United States Department of Agriculture (USDA), Natural Resources Conservation Service, 1986. The SCS technique has been upgraded to work with larger basins by weighting curve numbers related to watershed/basin area. This approach was originally designed to be applied to 15-km² basins (Hagras, 2023). Freely released

data and curves may be used to compute the CN, but it is challenging and time-consuming. Using RS and GIS techniques in conjunction with hydrologic processes allows for considerable cost and time savings with outstanding reliability and precision compared to traditional strategies. (Al-Ghobari et al., 2020). Equation (4) of the Weighted Curve Number (CN_w/CN_{II}) is given below:

$$CN_{II} = \frac{\sum (CN_i \times A_i)}{\sum A_i} \tag{4}$$

where; CN_{II} = Weighted curve number. CN_i = Curve number. A_i = Area with curve number CN_i .

2.3.2 Mann-Kendall method

Mann–Kendall is a non-parametric trend analysis method commonly used to detect trends in climatological and hydrological time series (Kendall, 1975; Mann, 1945). The Mann–Kendall test statistic S can be given as:

$$S_i = \sum_{i=1}^{n-1} \sum_{j=i+1}^n \text{sign}(x_j - x_i) \tag{5}$$

$$\text{Sign}(x_j - x_i) = \begin{cases} +1 & \text{if } (X_j - X_i) > 0 \\ 0 & \text{if } (X_j - X_i) = 0 \\ -1 & \text{if } (X_j - X_i) < 0 \end{cases} \tag{6}$$

where x_i and X_j are the ranked values of the data and n is the length of the data series for independent and identically distributed data, the statistic's variance is given as:

$$\text{Var}(S) = \frac{n(n-1)(2n+5) - \sum_{i=1}^m t_i(t_i-1)(2t_i+5)}{18} \tag{7}$$

where m is the number of ties values and t_i is the number of ties of extent i . The Mann–Kendall test statistic, Z_s , can be estimated as:

$$Z_s = \begin{cases} \frac{S-1}{\sqrt{\text{Var}(S)}}, & \text{if } S > 0 \\ 0, & \text{if } S = 0 \\ \frac{S+1}{\sqrt{\text{Var}(S)}}, & \text{if } S < 0 \end{cases} \tag{8}$$

In the data series, the positive Z value denotes a positive trend, while a negative value denotes a downward trend. The specific significance level ($=0.05$) is used for this test. Z_s is compared to $Z_{1-\alpha/2}$ to determine whether a trend is significant at that level. If $S > Z_{1-\alpha/2}$, the trend is significant. $Z_{1-\alpha/2}$ is derived from the normative cumulative distribution in this case.

3 Results and discussion

This study estimated the surface runoff of the Padma River basin using the SCS-CN method. The runoff-generating process is incredibly intricate, nonlinear, and dynamic, and it is impacted by a variety of interconnected physical factors. To effectively manage and develop water resources, a thorough runoff assessment was done. Every year in this basin, conditions resembling a drought occur because the basin receives below-average precipitation and suffers from excessive runoff as a result of unexpectedly heavy precipitation. According to the most recent research, agriculture is the primary land use class in the study area. Fallow land and open scrubland are two other types of land use that are crucial for surface runoff. When measuring soil, the hydrologic soil group, which represents soil character, category, and infiltration capability, is also extremely useful.

3.1 Land use land cover (LULC)

The amount of runoff used in this research, which is greatly influenced by land use and land cover (LULC) patterns in a given area, was made available by the Environmental Systems Research Institute (ESRI). The ESRI 10-m resolution

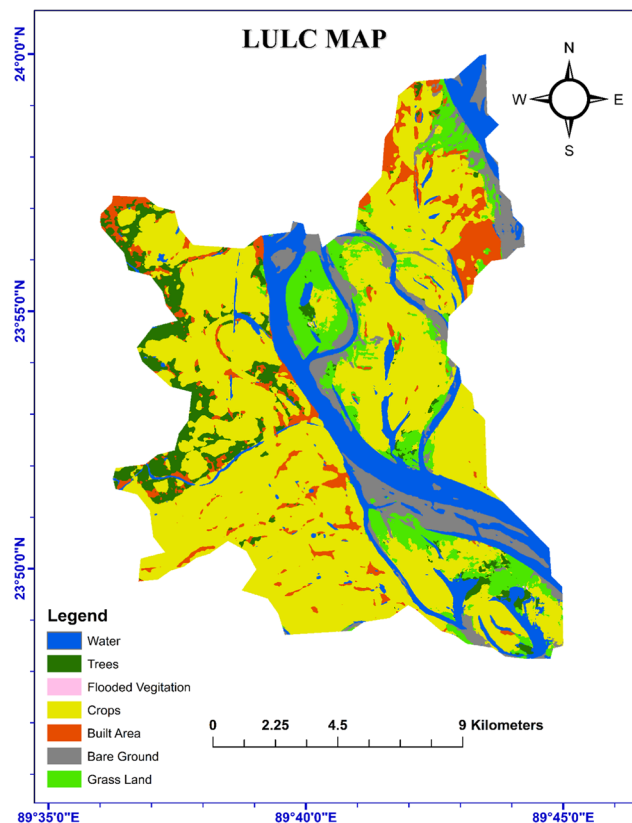
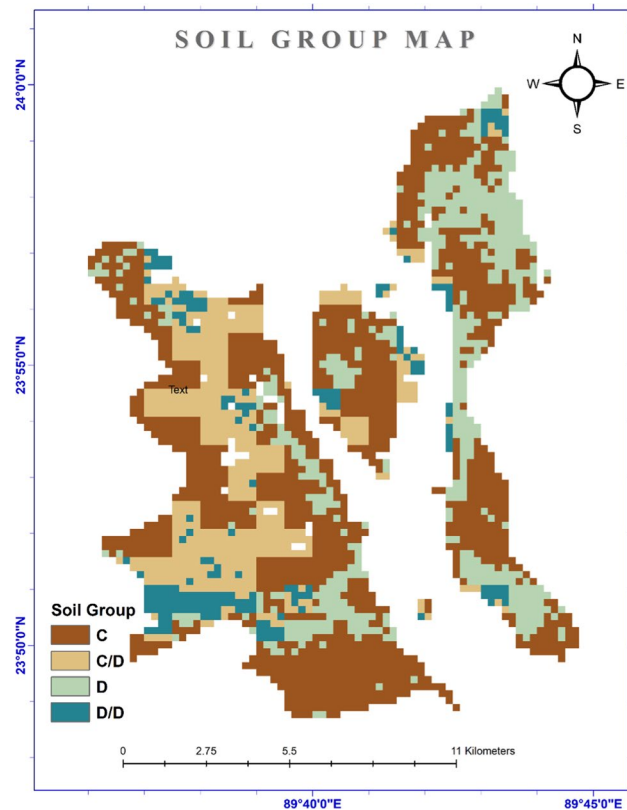


Fig. 2 Land use map of the study area

Table 2 Distribution Land use and land classes (LULC) in the basin

SN	LULC types	Area (km ²)	Area (%)
1	Water	25.95	14.50558
2	Trees	11.36	6.353231
3	Flooded Vegetation	0.02	0.012243
4	Crops	100.22	56.02886
5	Built Area	12.07	6.745412
6	Bare Ground	13.75	7.684021
7	Grass Land	15.51	8.670652

land-cover data is especially facilitated with classified land-cover details; this means the images are previously classified as per cover classes. However, the major LULC classes covered in the study area are trees, agricultural land, built-up areas, grassland, and water bodies. The details of land use and land cover in the study area are shown in Fig. 2 and Table 2. It can be seen that almost 100.22 km² (56.03%) of the Padma River basin area has been used for agricultural purposes. Trees comprised 11.3641 km² (6.35%) of the total area in the study area, with grassland covering almost 15.5 km² (8.67%). The flooded vegetation covers 0.022 km² (0.012%) of the land, and the bare ground covers 13.745 km² (7.68%). In the basin, the built-up area is 12.066 km² (6.75%), and river/water bodies are 25.946 km² (14.51%).

**Fig. 3** Hydrologic Soil Group map of the study area

3.2 Hydrologic soil group

The hydrologic soil group (HSG), computed through the soil texture classes, is the most important factor in the runoff process after LULC. The HSG map of the study area was generated using the Arc GIS software (Fig. 3). The HSG is divided into four groups based on the infiltration capacity of the surface soil, most likely A, B, C, and D. Table 3 presents the HSG categorization results as well as the soil classification criteria. With an area of 85.31 km² (52.22%) or more, hydrological soil group C covers the largest portion of the Padma River basin. Group D hydrological soil encompasses 11.88 km² (7.27%) of the research area, group C/D hydrological soil covers 32.25 km² (19.74%), and group D hydrological soil occupies 33.94 km² (20.77%).

3.3 Area weighted curve number

The HSG, LULC, hydrological condition, and antecedent moisture status (AMC), a dimensionless number runoff index, are used to determine the curve number (CN). Each soil type is allocated a hydrologic soil category of Group A, B, C, or D based on its infiltration properties. To qualify the magnitude of the curve number (CN), the required

Table 3 Distribution of hydrologic soil groups (HSG) in the study area

SN	HSG*	Soil Texture*	Runoff potential	Typical compositions (Ross et al., 2018)	Area (km ²)	Area (%)
1	C	Clay loam, Silty clay loam, Sandy clay loam, Loam, Silty loam, Silt	Moderately high	< 50% sand and 20–40% clay	1122.11	60.75
2	D	Clay, Silty clay, Sandy clay	High	< 50% sand and > 40% clay	4.87	0.26
3	C/D	Clay loam, Silty clay loam, Sandy clay loam, Loam, Silty loam, Silt	High	< 50% sand and 20–40% clay	711.67	38.54
4	D/D	Clay, Silty clay, Sandy clay	High	< 50% sand and > 40% clay	8.20	0.45

*Soil texture classes that typically comprise hydrologic soil groups (HSGs) (USDA, 2009)

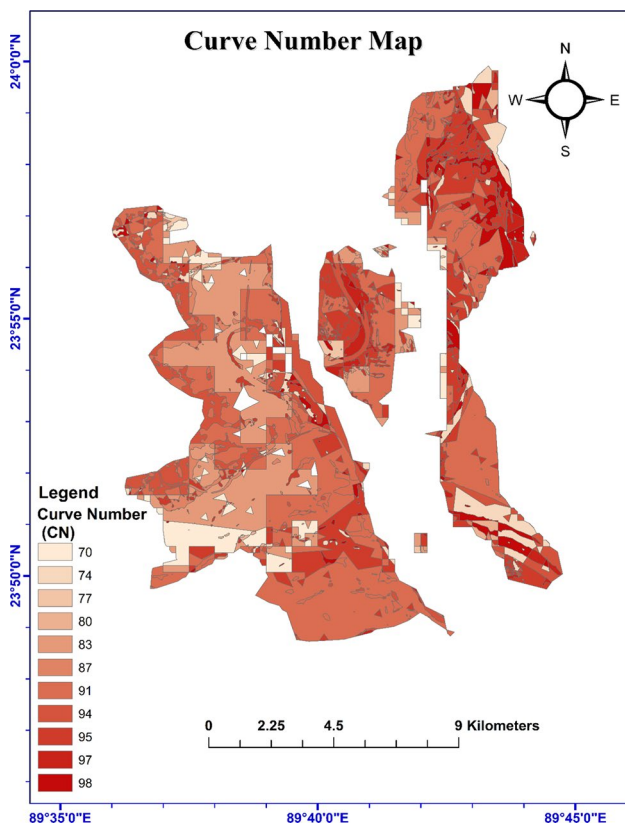


Fig. 4 Curve Number map of the study area

manipulation and overlay operations of the LULC class and the HSG were performed in the GIS platform. The values of CN typically fall between 1 and 100. Both Fig. 4 and Table 4 provide an in-depth explanation of the LULC and HSG's connections to the CN. The CN value has a direct correlation to the amount of runoff. An overlay analysis was carried out with Arc GIS 10.8 using a soil, land use, and hydrological soil group map to produce a new attribute table. This analysis was used to generate the table. The overall area-weighted curve number for the study region is calculated using the results from these HSGs and attribute tables. The minimum curve number that can be assigned to crops is 70, while the maximum curve number that can be assigned to water bodies is 98.

3.4 Rainfall analysis

There is a significant variation from year to year in the typical amount of precipitation that is received in this area. As a result of this, the investigation that is currently being carried out makes use of rainfall data ranging from 2010 to 2020. The highest annual average rainfall was recorded in 2020, with 3094.86 mm, while the lowest was recorded in 2012, with 1095.65 mm. There is very little room for doubt that the average annual rainfall in the studied area is steadily rising

Table 4 LULC and HSG and their corresponding CN values

SN	LULC	HSG	Area (km ²)	CN
1	Bare ground	C	2.94	97
2	Built area	C	6.99	91
3	Crops	C	38.95	91
4	Flooded vegetation	C	0.01	95
5	Grass land	C	3.98	95
6	Trees	C	6.80	94
7	Water	C	6.54	94
8	Bare ground	C/D	0.55	95
9	Built area	C/D	1.29	95
10	Crops	C/D	20.30	83
12	Grass land	C/D	0.62	83
13	Trees	C/D	1.95	87
14	Water	C/D	0.68	87
15	Bare ground	D	2.80	98
16	Built area	D	2.70	98
17	Crops	D	12.33	95
18	Grass land	D	2.41	95
19	Trees	D	0.86	74
20	Water	D	4.61	74
21	Bare ground	D/D	0.60	80
22	Built area	D/D	0.27	80
23	Crops	D/D	6.64	70
24	Flooded vegetation	D/D	0.00	70
25	Grass land	D/D	0.47	77
26	Trees	D/D	0.20	77
27	Water	D/D	0.71	98

as time passes. In addition, annual rainfall totals on average are also significantly higher than elsewhere in Bangladesh. There is a possibility that the variation in precipitation could be attributed to climate change.

3.5 Runoff assessment

The eleven-year's annual precipitation and runoff for the Padma River Basin can be found demonstrated in Fig. 5. The SCS-CN method was utilized to perform the runoff computation in this study. The river basin's annual runoff averaged 409.67 mm from 2010 to 2020, with the highest runoff recorded in 2017 at 1040.74 mm and the lowest runoff recorded in 2017 at 91.83 mm. The average annual rainfall in the study area is 4506.45 mm, which represents 22.25% of the annual runoff volume.

3.6 Autocorrelation

It is necessary to specify the autocorrelation characteristics of the runoff data series before making a decision regarding the trend detection test. A perfect positive

Fig. 5 Yearly rainfall-runoff variation over 10 years (2011–2020)

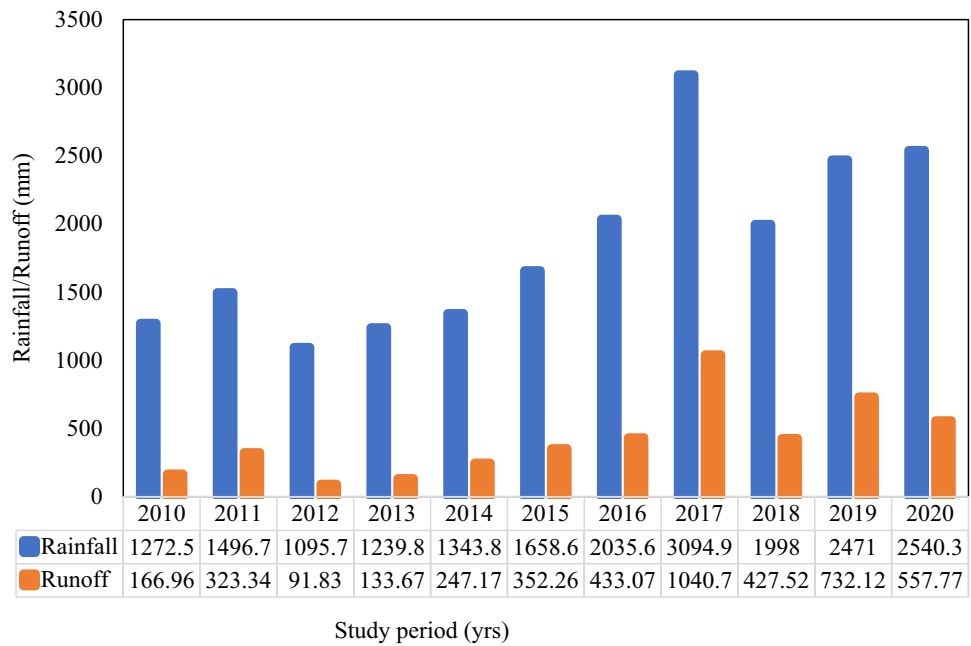
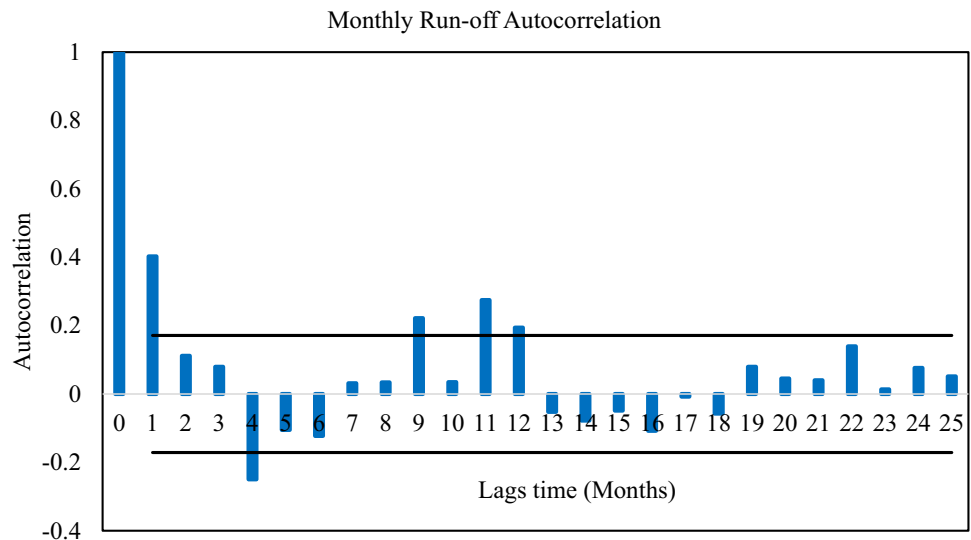


Fig. 6 Autocorrelation function for different lags of monthly runoff



correlation is represented by an autocorrelation of +1 (an increase seen in one time series leads to a proportionate increase in the other time series), and a perfect negative correlation is represented by an autocorrelation of -1 (an increase observed in one time series results in a proportionate decrease in the other time series) (Tim Smith, 2023). Figure 6 shows an autocorrelation of the monthly surface runoff of the study area. The lag time of the monthly runoff is represented by the abscissa, while the autocorrelation is shown by the ordinate. Here, we can see that there is a big spike at lag 1 and considerably smaller spikes for the subsequent lags. Lag times 4 to 6 and 13 to 18 have been observed to have negative

autocorrelation. On the other hand, positive autocorrelation has been observed for all the other lag times. Based on the findings of the analysis, it can be seen that almost all of the autocorrelations are found to be within the 95% confidence limit. A few lags fall outside the 95% certainty confidence limit. According to this research, across all monthly runoff amounts at different periods, there is non-significant autocorrelation. Rainfall data with daily, monthly, seasonal, and yearly temporal levels were associated for both significant and non-significant autocorrelations analysis (Rashid et al., 2013).

Fig. 7 Monthly deviation from average surface runoff amounts in the watershed

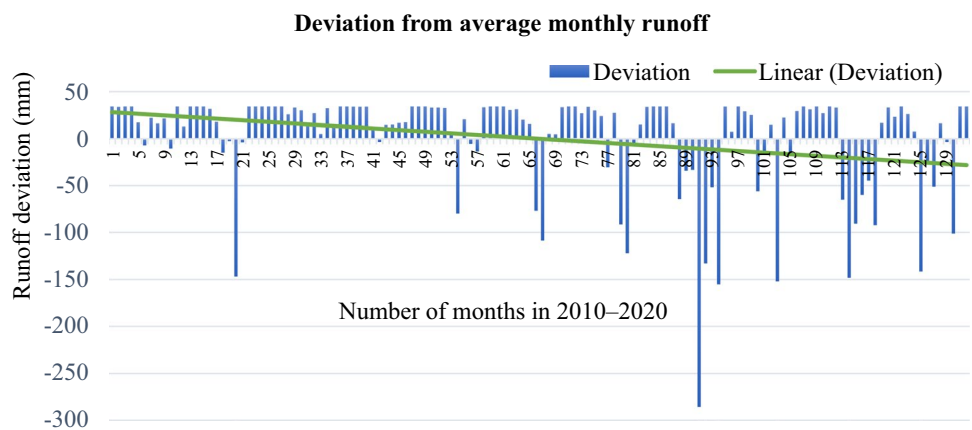


Table 5 Mann–Kendall trend and Sen slope analysis

Man-Kendall trend ($\alpha=5\%$)	H_0 hypothesis ($\alpha=5\%$)	Kendall's tau	p -value (Two-tailed)	Sen's slope
Yes	Rejected	0.18	0.002	0.08

was measured at 285.69 mm in July 2016, then decreased to 155.16 mm in October of the same year. Therefore, during the period that was analyzed for the watershed, no discernible changes in the trend line for the monthly runoff were seen to have a statistically significant impact. The basin's monthly flow was decreasing, with a Sen slope of approximately 0.08, according to the findings (Fig. 7).

3.7 Monthly runoff trend

From 2010 to 2020, a trend analysis of the monthly surface runoff for the Padma River basin was carried out. The monthly values demonstrated that runoff varies with the seasons, with most of the values being high from May until September. The majority of the high values occurred during this period. The runoff reached its maximum during these months, then began to decline. The height runoff deviation

3.8 Mann–Kendall trend analysis

The Mann–Kendall test reveals whether there are monotonic trends in either a positive or negative direction. This technique was used to find any monotonic trends that might have been present in the runoff data series. The outcome of the Mann–Kendall test and Sen slope analysis of the monthly runoff patterns are shown in Table 5. The test's null (H_0) or alternative (H_1) hypotheses are indicated by

Fig. 8 Mann–Kendall trend and Sen slope analysis from surface runoff amounts

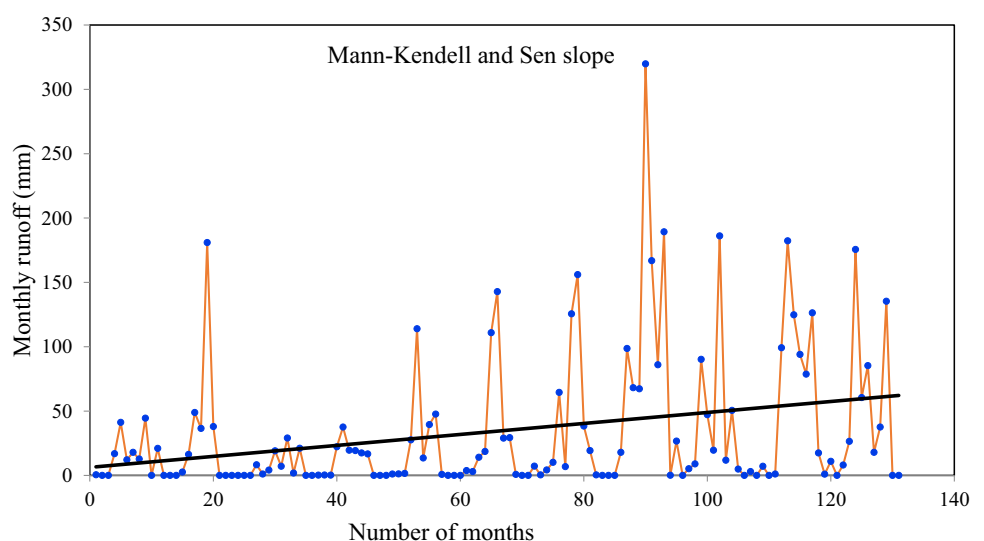
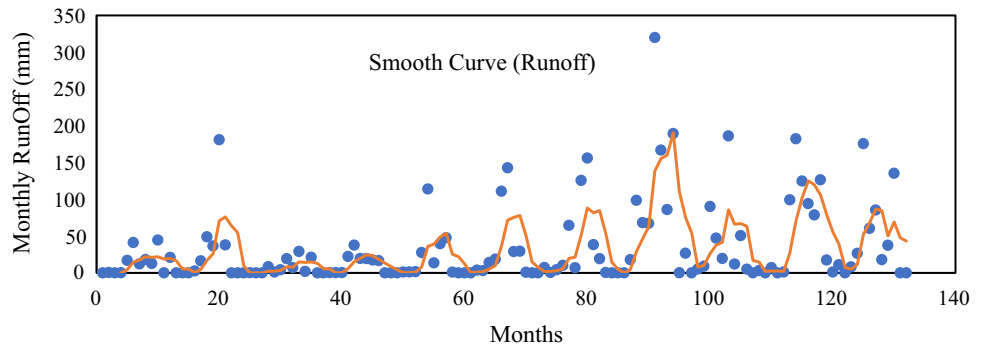


Fig. 9 Runoff and smoothing curve of the basin



the two-tailed p -value. The alternative hypothesis suggests an increasing or declining trend in the runoff data series if the null hypothesis is rejected. The p -value was higher than the 0.05 criterion of significance. Because the p -value was greater than the significance level, it demonstrated that the null hypothesis was rejected and the alternative hypothesis was accepted. Accordingly, it was statistically significant for this watershed that there were both decreasing and growing tendencies. This watershed's Sen slope value of 0.08 indicates runoff trending uphill Table 5. One should reject the null hypothesis H_0 and accept the alternative hypothesis H_a since the computed p -value exceeds the significance level ($\alpha = 5\%$). Less than 0.22% of the time, the null hypothesis H_0 is rejected even when true. Figure 8 presents the graphical look of the Mann-Kendell test and Sen Slope.

3.9 Smooth curve and runoff potentiality

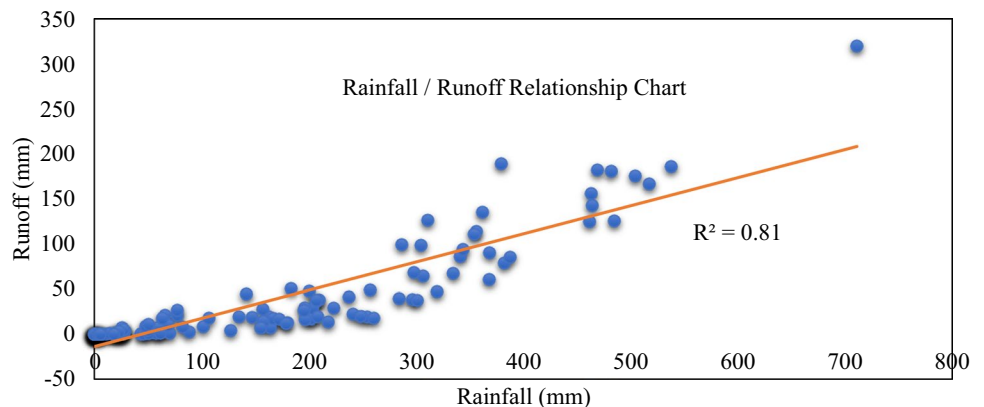
The runoff from the study area is shown as an undulating curve in Fig. 9. It demonstrates that while the runoff levels fluctuated from peak to peak, all peaks occurred between May to September, when most of the rainfall took place. This analysis suggests that the runoff has features that manifest as varying degrees of effect for the study area. A

solid correlation between the two criteria was shown by the basin's anticipated monthly rainfall-runoff relation (Fig. 10) and a linear relationship was discovered between monthly rainfall and runoff ($R^2 = 0.811$). According to this analysis, the SCS-CN approach can be used to predict the surface runoff resulting from the rainfalls in the Padma River basin.

3.10 Discussion

The study aim was to identify runoff levels in the years 2010–2020 using the GIS-based SCS-CN method in the study area. Rainfall intensity changes can have a significant impact on the parameters of the model used to estimate runoff (Wang & Bi, 2020). In 2012, the lowest rainfall was observed, and therefore the lowest runoff was estimated in the study area. In terms of monthly rainfall-runoff condition in this year, the maximum rainfall and runoff occurred from July to September. In November, although the rainfall was relatively low, the runoff was estimated to be substantially higher due to the fact that there were six consecutive days with heavy rainfall during the first week of this month. In November, although the rainfall was relatively low, the runoff was estimated to be substantially higher due to the fact that there were six consecutive days with heavy rainfall during the first

Fig. 10 Estimated monthly rainfall-runoff relationship



week of this month. On the other hand, over the study period, the maximum yearly rainfall and runoff were found in 2017, and they were followed by the rainfall and runoff of the year 2019. Notably, in 2017, there was high rainfall throughout the year except for January and February; especially, the consistently continuous rainfall received during July resulted in a substantial amount of runoff. Nevertheless, the rainfall in 2019 was found to be comparatively lower than that of 2020, and the resulting runoff was estimated to be higher owing to the consistent rainfall pattern over the year in 2019.

The amount and timing of runoff were found to be significantly influenced by the physiographic factor, particularly the LULC change dynamics, in addition to the climatological element (Khazr et al., 2022). Since LULC changes have significantly converted forests to agriculture or urban areas, as well as changes in the type of vegetation cover, such as deforestation or reforestation. Therefore, these changes greatly alter the way water moves through the landscape, affecting the amount of runoff, infiltration, and evapotranspiration (Das et al., 2018). There was less urban and high-slope terrain in this study; thus, the average runoff was correspondingly lower (Radwan et al., 2020).

Overall, the use of a GIS and RS platform in the SCS-CN approach for runoff assessment in the Padma River basin provided crucial information for water management and planning efforts in the region (Satheshkumar et al., 2017b). It is essential to clearly figure out the factors that directly influence the quantity quality and timing of the runoff to maintain the environmental flow to the river and to safe guard the riverine that are most at risk (Kuriqi et al., 2019). Decision-makers however, can take proactive measures to protect human lives, infrastructure, and overall ecosystem from the impacts of water-related hazards.

4 Conclusions

In this study, the SCS-CN model was combined with GIS techniques to figure out how much water could run off the surface. Several meteorological, topsoil textural, and spatial data, such as precipitation, soil texture and types, land use and land-cover classes, were taken into account as important input parameters to the SCS-CN model. Here, GIS was therefore used to perform some robust chores like integrating and interpreting all input and output parameters and plotting them alone with their spatial and temporal distribution. Based on the texture classes and hydrological condition, the soil in this area primarily belonged to the C, D, C/D, and D/D soil groups. The area average weighted curve number of the entire watershed was determined considering a variety of sub-catchments with various CNs. For the hydrological

soil groups C, D, C/D, and D/D, it is advised that weighted curve numbers be used since this will result in less variation in CN values between the groups. For proper surface runoff, the distributed CN value considers hydrological soil groups. The monthly runoff patterns over the study period were analyzed using autocorrelation, Mann–Kendall, and Sen slope estimation techniques. The Mann–Kendall test indicated a significant difference in this watershed, and it revealed a trend with a Sen slope of 0.08; it also indicated that these runoff data series exhibited a substantial trend. Even though the seasonal changes in the runoff value were noticed due to the discrete pattern of the runoff data set, the overall surface runoff over the time of the study was shown by a smooth curve. These curves shifted due to the seasonal variation in monsoonal rainfall. Most of the curve's highest peaks occurred between May and September when precipitation peaked. The monthly mean runoff, determined using smoothing curves, has a value of 34 mm. Surface runoff transports about 26% of the water from rainfall directly to the river. This trend and water volume directly reveal the distribution and contribution of rainwater. Planning the management of surface water and the potential and contribution of groundwater recharge may benefit from it.

However, it indeed appears true that the surface runoff estimation in a watershed or at some greater spatial scale has always been found to be challenging, especially where there is a scarcity of the necessary reliable data required to run a runoff model. The accuracy and reliability of the estimated runoff results depend on the spatial and temporal resolution of the input data set. The higher the resolution of the data, the more accurate and reliable the results will be. The volume of runoff in a river basin can only be accurately estimated with knowledge of the rainfall, land use, and soil types. To predict and measure runoff, it is important to consider factors for rainfall, such as intensity, duration, and dispersion. Various storm and drainage features, basin size, topography, and other elements influence the interplay between rainfall and runoff. It is important to assign the right CN value to each land use and soil attribute to measure runoff in each land use class. Although estimating the runoff in a very large basin, such as the Padma basin in Bangladesh, was rather difficult, the result was improved by dividing river basins into smaller watershed zones where there was more control over database construction and analysis. In the monsoon and pre-monsoon seasons, the humid Padma River basin receives unusually strong rainfall and occasionally encounters flash floods. In addition, irregular and insufficient precipitation, floods, soil erosion brought on by heavy rains, and a rapid rate of surface drainage are all frequent occurrences. The above data could be combined with our most recent research to produce an appropriate amount of runoff and a scenario for comprehending and managing water resources in the study area. This could be seen as a

future extension of the current study's work, which could lead to better results.

Acknowledgements The authors are thankful to NASA and ESRI for providing the necessary data. The authors would like to thank the Institute of Water and Environment (DUET) for its constant support and wonderful research platform.

Author contributions MTA: writing, visualization, data curation, MRI*: conceptualisation, methodology, MZK: visualization, data curation, HMI: editing, MMM: visualization, data curation, MRI:resources, MS:resources,editing

Data availability The datasets used in this study will be available upon reasonable request.

Declarations

Conflict of interest The authors declare no competing interests.

References

- Al-Ani, T., Habib, I., Abdulaziz, A., & Ouda, N. (1971). Plant indicators in Iraq: II. Mineral composition of native plants in relation to soils and selective absorption. *Plant and Soil*, *35*, 29–36. <https://doi.org/10.1007/BF01372629>
- Al-Ghobari, H., Dewidar, A., & Alataway, A. (2020). Estimation of surface water runoff for a semi-arid area using RS and GIS-based SCS-CN method. *Water*, *12*(7), 1924. <https://doi.org/10.3390/w12071924>
- Al-Ghobari, H., & Dewidar, A. Z. (2021). Integrating GIS-Based MCDA Techniques and the SCS-CN Method for Identifying Potential Zones for Rainwater Harvesting in a Semi-Arid Area. *Water*, *13*(5), 704. <https://doi.org/10.3390/w13050704>
- Arefin, R., Meshram, S., & Seker, D. (2021). River channel migration and land-use/land-cover change for Padma River at Bangladesh: a RS-and GIS-based approach. *International Journal of Environmental Science and Technology*, 1–18. <https://doi.org/10.1007/s13762-020-03063-7>
- Bal, M., Dandpat, A. K., & Naik, B. (2021). Hydrological modeling with respect to impact of land-use and land-cover change on the runoff dynamics in Budhabalanga river basing using ArcGIS and SWAT model. *Remote Sensing Applications: Society and Environment*, *23*, 100527. <https://doi.org/10.1016/j.rsase.2021.100527>
- Balkhair, K. S., & Ur Rahman, K. (2021). Development and assessment of rainwater harvesting suitability map using analytical hierarchy process, GIS and RS techniques. *Geocarto International*, *36*(4), 421–448. <https://doi.org/10.1080/10106049.2019.1608591>
- Bera, A., & Singh, S. K. (2021). Comparative Assessment of Livelihood Vulnerability of Climate Induced Migrants: A Micro Level Study on Sagar Island, India. *Sustainability, Agri, Food and Environmental Research*, *9*(2). <https://doi.org/10.7770/safer-V9N2-art2324>
- Bhat, M. S., Alam, A., Ahmad, B., Kotlia, B. S., Farooq, H., Taloor, A. K., & Ahmad, S. (2019). Flood frequency analysis of river Jhelum in Kashmir basin. *Quaternary International*, *507*, 288–294. <https://doi.org/10.1016/j.quaint.2018.09.039>
- Caletka, M., Šulc Michalková, M., Karásek, P., & Fučík, P. (2020). Improvement of SCS-CN initial abstraction coefficient in the Czech Republic: a study of five catchments. *Water*, *12*(7), 1964. <https://doi.org/10.3390/w12071964>
- Das, P., Behera, M. D., Patidar, N., Sahoo, B., Tripathi, P., Behera, P. R., Srivastava, S., Roy, P. S., Thakur, P., & Agrawal, S. (2018). Impact of LULC change on the runoff, base flow and evapotranspiration dynamics in eastern Indian river basins during 1985–2005 using variable infiltration capacity approach. *Journal of Earth System Science*, *127*, 1–19. <https://doi.org/10.1007/s12040-018-0921-8>
- Deshmukh, D. S., Chaube, U. C., Hailu, A. E., Gudeta, D. A., & Kassa, M. T. (2013). Estimation and comparison of curve numbers based on dynamic land use land cover change, observed rainfall-runoff data and land slope. *Journal of Hydrology*, *492*, 89–101. <https://doi.org/10.1016/j.jhydrol.2013.04.001>
- Farooq, M., Singh, S. K., & Kanga, S. (2021). Mainstreaming adaptation strategies in relevant flagship schemes to overcome vulnerabilities of climate change to agriculture sector. *Res. J. Agri. Sci.: Int. J.*, *12*, 637–646.
- Fausey, N. (2004). Drainage, surface and subsurface. *Encyclopedia of Soils in the Environment*, 409–413.
- Hagras, A. (2023). Runoff modeling using SCS-CN and GIS approach in the Tayiba Valley Basin, Abu Zenima area, South-west Sinai, Egypt. *Modeling Earth Systems and Environment*. <https://doi.org/10.1007/s40808-023-01714-5>
- Ibrahim, A., Zakaria, N., Harun, N., & Hashim, M. M. M. (2021). Rainfall runoff modeling for the basin in Bukit Kledang, Perak. IOP Conference Series: Materials Science and Engineering,
- Islam, A. R. M. T., Talukdar, S., Mahato, S., Ziaul, S., Eibek, K. U., Akhter, S., Pham, Q. B., Mohammadi, B., Karimi, F., & Linh, N. T. T. (2021). Machine learning algorithm-based risk assessment of riparian wetlands in Padma River Basin of Northwest Bangladesh. *Environmental Science and Pollution Research*, *28*, 34450–34471. <https://doi.org/10.1007/s11356-021-12806-z>
- Jaafar, H. H., Ahmad, F. A., & El Beyrouthy, N. (2019). GCN250, new global gridded curve numbers for hydrologic modeling and design. *Scientific data*, *6*(1), 1–9. <https://doi.org/10.1038/s41597-019-0155-x>
- Jahan, K., Pradhanang, S. M., & Bhuiyan, M. A. E. (2021). Surface Runoff Responses to Suburban Growth: An Integration of Remote Sensing, GIS, and Curve Number. *Land*, *10*(5), 452. <https://doi.org/10.3390/land10050452>
- Karimi, H., & Zeinivand, H. (2021). Integrating runoff map of a spatially distributed model and thematic layers for identifying potential rainwater harvesting suitability sites using GIS techniques. *Geocarto International*, *36*(3), 320–339. <https://doi.org/10.1080/10106049.2019.1608590>
- Kendall, M. (1975). *Rank Correlation Methods* (4th ed.). Charles Griffin.
- Khazr, B. O., Ibrahim, G. R. F., Hamid, A. A., & Ail, S. A. (2022). Run-off estimation using SCS-CN and GIS techniques in the Sulaymaniyah sub-basin of the Kurdistan region of Iraq. *Environment, Development and Sustainability*, *24*(2), 2640–2655. <https://doi.org/10.1007/s10668-021-01549-z>
- Kumar, T., & Jhariya, D. (2017). Identification of rainwater harvesting sites using SCS-CN methodology, remote sensing and Geographical Information System techniques. *Geocarto International*, *32*(12), 1367–1388. <https://doi.org/10.1080/10106049.2016.1213772>
- Kumar, A., Kanga, S., Taloor, A. K., Singh, S. K., & Đurin, B. (2021). Surface runoff estimation of Sind river basin using integrated SCS-CN and GIS techniques. *HydroResearch*, *4*, 61–74. <https://doi.org/10.1016/j.hydres.2021.08.001>
- Kuriqi, A., Pinheiro, A. N., Sordo-Ward, A., & Garrote, L. (2019). Influence of hydrologically based environmental flow methods on flow alteration and energy production in a run-of-river hydropower plant. *Journal of Cleaner Production*, *232*, 1028–1042. <https://doi.org/10.1016/j.jclepro.2019.05.358>
- Lian, H., Yen, H., Huang, J.-C., Feng, Q., Qin, L., Bashir, M. A., Wu, S., Zhu, A.-X., Luo, J., & Di, H. (2020). CN-China: Revised runoff curve number by using rainfall-runoff events data in China.

- Water Research*, 177, 115767. <https://doi.org/10.1016/j.watres.2020.115767>
- Ling, L., Yusop, Z., Yap, W.-S., Tan, W. L., Chow, M. F., & Ling, J. L. (2020). A calibrated, watershed-specific SCS-CN method: application to Wangjiaqiao watershed in the Three Gorges area, China. *Water*, 12(1), 60. <https://doi.org/10.3390/w12010060>
- Lobo, M., Clements, D. L., & Widana, N. (2004). Infiltration from irrigation channels into soil with impermeable inclusions. *ANZIAM Journal*, 46, C1055-C1068. <https://doi.org/10.21914/anziamj.v46i0.1006>
- Mann, H. (1945). Spatial-temporal variation and protection of wetland resources in Xinjiang. *Econometrica*, 13, 245–259. <https://doi.org/10.1007/s12665-018-7764-0>
- Ogden, F. L., Hawkins, R. P., Walter, M. T., & Goodrich, D. C. (2017). Comment on “Beyond the SCS-CN method: A theoretical framework for spatially lumped rainfall-runoff response” by MS Bartlett et al. *Water Resources Research*, 53(7), 6345–6350. <https://doi.org/10.1002/2015WR018439>
- Pandey, A. C., Singh, S. K., Nathawat, M., & Saha, D. (2013). Assessment of surface and subsurface waterlogging, water level fluctuations, and lithological variations for evaluating groundwater resources in Ganga Plains. *International Journal of Digital Earth*, 6(3), 276–296. <https://doi.org/10.1080/17538947.2011.624644>
- Pastor, A., Ludwig, F., Biemans, H., Hoff, H., & Kabat, P. (2013). Accounting for environmental flow requirements in global water assessments. *Hydrology & Earth System Sciences Discussions*, 10(12). <https://doi.org/10.5194/hess-18-5041-2014>
- Piacentini, T., Galli, A., Marsala, V., & Miccadei, E. (2018). Analysis of soil erosion induced by heavy rainfall: A case study from the NE Abruzzo Hills Area in Central Italy. *Water*, 10(10), 1314. <https://doi.org/10.3390/w10101314>
- Radwan, F., Alazba, A., & Mossad, A. (2020). Analyzing the geomorphometric characteristics of semiarid urban watersheds based on an integrated GIS-based approach. *Modeling Earth Systems and Environment*, 6, 1913–1932. <https://doi.org/10.1007/s40808-020-00802-0>
- Rahman, S. A. Z., Mitra, K. C., & Islam, S. M. (2018). Soil classification using machine learning methods and crop suggestion based on soil series. 2018 21st International Conference of Computer and Information Technology (ICCIT),
- Raihan, F., Beaumont, L. J., Maina, J., Saiful Islam, A., & Harrison, S. P. (2020). Simulating streamflow in the Upper Halda Basin of southeastern Bangladesh using SWAT model. *Hydrological Sciences Journal*, 65(1), 138–151. <https://doi.org/10.1080/0262667.2019.1682149>
- Raihan, F., Ondrasek, G., Islam, M. S., Maina, J. M., & Beaumont, L. J. (2021). Combined Impacts of Climate and Land Use Changes on Long-Term Streamflow in the Upper Halda Basin, Bangladesh. *Sustainability*, 13(21), 12067. <https://doi.org/10.3390/su132112067>
- Rana, V. K., & Suryanarayana, T. M. V. (2020). GIS-based multi criteria decision making method to identify potential runoff storage zones within watershed. *Annals of GIS*, 26(2), 149–168. <https://doi.org/10.1080/19475683.2020.1733083>
- Rashid, M., Beecham, S., & Chowdhury, R. (2013). Assessment of statistical characteristics of point rainfall in the Onkaparinga catchment in South Australia. *Hydrology and Earth System Sciences Discussion*, 10(5), 5975–6017. <https://doi.org/10.5194/hessd-10-5975-2013>
- Renard, K. G., Foster, G., Yoder, D., & McCool, D. (1994). RUSLE revisited: Status, questions, answers, and the future. *Journal of Soil and Water Conservation*, 49(3), 213–220.
- Rizeei, H. M., Pradhan, B., & Saharkhiz, M. A. (2018). Surface runoff prediction regarding LULC and climate dynamics using coupled LTM, optimized ARIMA, and GIS-based SCS-CN models in tropical region. *Arabian Journal of Geosciences*, 11(3), 1–16. <https://doi.org/10.1007/s12517-018-3397-6>
- Ross, C., Prihodko, L., Anchang, J., KUMAR, S., Ji, W., & Hanan, N. (2018). Global hydrologic soil groups (HYSOGs250m) for curve number-based runoff modeling. *ORNL DAAC*. <https://doi.org/10.3334/ORNLDAAC/1566>
- Satheeshkumar, S., Venkateswaran, S., & Kannan, R. (2017b). Rainfall-runoff estimation using SCS-CN and GIS approach in the Pappiredipatti watershed of the Vaniyar sub basin, South India. *Modeling Earth Systems and Environment*, 3, 1–8. <https://doi.org/10.1007/s40808-017-0301-4>
- Satheeshkumar, S., Venkateswaran, S., & Kannan, R. (2017a). Rainfall-runoff estimation using SCS-CN and GIS approach in the Pappiredipatti watershed of the Vaniyar sub basin, South India. *Modeling Earth Systems and Environment*, 3(1), 24. <https://doi.org/10.1007/s40808-017-0301-4>
- Shadeed, S., & Almasri, M. (2010). Application of GIS-based SCS-CN method in West Bank catchments, Palestine. *Water Science and Engineering*, 3(1), 1–13. <https://doi.org/10.3882/j.issn.1674-2370.2010.01.001>
- Shao, Z., Fu, H., Li, D., Altan, O., & Cheng, T. (2019). Remote sensing monitoring of multi-scale watersheds impermeability for urban hydrological evaluation. *Remote Sensing of Environment*, 232, 111338. <https://doi.org/10.1016/j.rse.2019.111338>
- Shi, W., & Wang, N. (2020). An improved SCS-CN method incorporating slope, soil moisture, and storm duration factors for runoff prediction. *Water*, 12(5), 1335. <https://doi.org/10.3390/w12051335>
- Silva, C., & Oliveira, C. (1999). Runoff measurement and prediction for a watershed under natural vegetation in central Brazil. *Revista brasileira de ciência do solo*, 23, 695–701. <https://doi.org/10.1590/S0100-06831999000300024>
- Soruco, A., Vincent, C., Rabatel, A., Francou, B., Thibert, E., Sicart, J. E., & Condom, T. (2015). Contribution of glacier runoff to water resources of La Paz city, Bolivia (16 S). *Annals of Glaciology*, 56(70), 147–154. <https://doi.org/10.3189/2015AoG70A001>
- Soulis, K. X. (2021). Soil Conservation Service Curve Number (SCS-CN) Method: Current Applications, Remaining Challenges, and Future Perspectives. In (Vol. 13, pp. 192): Multidisciplinary Digital Publishing Institute.
- Tim Smith, C. M., Patrice Williams. (2023, February 11, 2023). *Autocorrelation: What It Is, How It Works, Tests*. Investopedia. Retrieved March 6 from <https://www.investopedia.com/terms/a/autocorrelation.asp>
- USDA, N. (1999). United States department of agriculture. Natural Resources Conservation Service. Plants Database. <http://plants.usda.gov> (accessed in 2000). <https://doi.org/10.1002/ps.684>
- Verma, S., Singh, P., Mishra, S., Singh, V., Singh, V., & Singh, A. (2020a). Activation soil moisture accounting (ASMA) for runoff estimation using soil conservation service curve number (SCS-CN) method. *Journal of Hydrology*, 589, 125114. <https://doi.org/10.1016/j.jhydrol.2020.125114>
- Verma, S., Mishra, S., & Verma, R. (2020a). Improved runoff curve numbers for a large number of watersheds of the USA. *Hydrological Sciences Journal*, 65(16), 2658–2668. <https://doi.org/10.1080/02626667.2020.1832676>
- Verma, S., Singh, P., Mishra, S. K., Singh, V., Singh, V., & Singh, A. (2020b). Activation soil moisture accounting (ASMA) for runoff estimation using soil conservation service curve number (SCS-CN) method. *Journal of Hydrology*, 589, 125114. <https://doi.org/10.1016/j.jhydrol.2020.125114>
- Verma, R. K., Verma, S., Mishra, S. K., & Pandey, A. (2021). SCS-CN-Based Improved Models for Direct Surface Runoff Estimation from Large Rainfall Events. *Water Resources Management*, 35(7), 2149–2175. <https://doi.org/10.1007/s11269-021-02831-5>
- Walega, A., Amatya, D. M., Caldwell, P., Marion, D., & Panda, S. (2020). Assessment of storm direct runoff and peak flow rates

- using improved SCS-CN models for selected forested watersheds in the Southeastern United States. *Journal of Hydrology: Regional Studies*, 27, 100645. <https://doi.org/10.1016/j.ejrh.2019.100645>
- Wang, X., & Bi, H. (2020). The effects of rainfall intensities and duration on SCS-CN model parameters under simulated rainfall. *Water*, 12(6), 1595. <https://doi.org/10.3390/w12061595>
- Zehtabiyani-Rezaie, N., Alvandifar, N., Saffaraval, F., Makkiabadi, M., Rahmati, N., & Saffar-Avval, M. (2019). A solar-powered solution for water shortage problem in arid and semi-arid regions in coastal countries. *Sustainable Energy Technologies and Assessments*, 35, 1–11. <https://doi.org/10.1016/j.seta.2019.05.015>

Springer Nature or its licensor (e.g. a society or other partner) holds exclusive rights to this article under a publishing agreement with the author(s) or other rightsholder(s); author self-archiving of the accepted manuscript version of this article is solely governed by the terms of such publishing agreement and applicable law.